Improved United Atom Force Field for Poly(dimethylsiloxane)

Amalie L. Frischknecht* and John G. Curro

Sandia National Laboratories, Albuquerque, New Mexico 87185

Received October 22, 2002; Revised Manuscript Received January 3, 2003

ABSTRACT: We develop a new united atom force field for computer simulations of poly(dimethylsiloxane) (PDMS) melts. The model is based on an explicit atom, class II potential studied previously. The effects of partial charges on the intermolecular structure are found to be stronger in the united atom model than in the explicit atom model, due to the lack of explicit hydrogen atoms. By adjusting the partial charges of the united atom force field, we obtain reasonable agreement with the results of the explicit atom model for the intermolecular structure, the pressure, and the chain dimensions in the melt.

Introduction

Silicone polymers such as poly(dimethylsiloxane) (PDMS) are very useful for engineering applications such as elastomeric seals, adhesives, coatings, and encapsulants due to their material properties. PDMS has one of the lowest glass transition temperatures of known polymers and is stable at relatively high temperatures. In many applications, PDMS exists near a surface in the amorphous liquid state or as a cross-linked network. Understanding in detail such issues as adhesive failure requires a molecular level understanding of the structure of the PDMS liquid. Molecular dynamics (MD) simulations are ideal for such studies, but they require an accurate force field for the polymer as input.

A recent study of the structure of PDMS melts compared results from wide-angle X-ray scattering, molecular dynamics simulation, and polymer reference interaction site theory (PRISM).[1] It was found that MD simulations using an explicit atom (EA), class II force field of Sun, Rigby, and others[2−6] gave excellent agreement with the experimental structure factor, whereas a united atom (UA) model of Sok and co-workers[7] was found to give poor agreement at low wave vectors, due to the model's inability to predict the correct PVT properties. It is desirable to have a good united atom force field for PDMS, since simulations with a united atom potential are considerably faster than explicit atom simulations. Our goal in this paper is to develop an improved united atom force field for PDMS, which captures as much as possible the features of the explicit atom model studied previously.

For the remainder of the paper, the explicit atom class II model will be referred to as EA/CII, the united atom class I model of Sok et al. will be referred to as UA/CI, and the new united atom model developed here will be referred to as the hybrid/UA model, for reasons described below. We describe the new model and the molecular dynamics simulations in section II and present results and comparisons to the previous work in section III.

II. Model and Molecular Dynamics

PDMS consists of a silicon−oxygen backbone, with two methyl groups attached to each silicon atom. United atom models treat each methyl group as a single atom, thus reducing the number of atoms per monomer from ten to four. To develop an improved united atom model, we implemented as much of the EA/CII potential as was possible within a united atom framework.

For the bond, angle, and torsional potentials we use the usual form of class I intramolecular potentials. The bond lengths vary around the preferred bond length r_0 in a harmonic potential

$$V_b(r) = k_b(r - r_0)^2 \tag{1}$$

as do the bond angles about a fixed angle θ_0:

$$V_a(\theta) = k_\theta(\theta - \theta_0)^2 \tag{2}$$

The torsional bond angles ϕ are subject to the torsional potential

$$V_t(\phi) = k_t[1 + \cos(n\phi)] \tag{3}$$

where the trans state corresponds to $\phi = \pi$. In addition to the potentials of eqs 1−3, the EA/CII force field contains several other terms, such as anharmonic bond and angle potentials and cross-terms such as bond−angle interactions. We ignore these extra terms but make an attempt to match the intramolecular potentials of eqs 1−3 in the hybrid/UA model to the corresponding bond−bond, angle−angle, and torsion−torsion potentials in the EA/CII model. We used the EA/CII values of r_0 for the bonds, in which case we find that the harmonic bond potential in eq 1 gives a good fit to the anharmonic EA/CII bond−bond potential, using the same values of k_b as in the UA/CI model.[7]

It was found in ref 1 that the bond angles in the condensed melt phase of PDMS are considerably renormalized from their hypothetical gas-phase values, which are used in the EA/CII potential. Here we chose to use the renormalized values shown in Table 1, as obtained from the MD simulations of ref 1, for the equilibrium bond angles θ_0. These values are in fact similar to the values used by Sok et al.[7] We chose to use the UA/CI values of Sok et al. for the k_θ. These values result in a similar steepness to the potential for the O−Si−O and C−Si−C angles as the EA/CII anharmonic potentials but give steeper potentials for the Si−O−Si and O−Si−C angles. We feel however this is justified since we are using the renormalized values for the equilibrium

* Corresponding author: e-mail alfrisc@sandia.gov.

10.1021/ma025763g CCC: $25.00
Published on Web 02/22/2003

Table 1. Intramolecular Potential Parameters for the Hybrid/UA and UA/CI Models

bonds	hybrid/UA: r_0 [Å]	k_b [kcal/(mol Å^2)]	UA/CI: r_0 [Å]	k_b [kcal/(mol Å^2)]
Si−O	1.64	350.12	1.60	350.12
Si−CH_3	1.90	189.65	1.88	189.65
angles	**hybrid/UA: θ_0 [deg]**	**k_θ [kcal/(mol deg^2)]**	**UA/CI: θ_0 [deg]**	**k_θ [kcal/(mol deg^2)]**
Si−O−Si	146.46	14.14	144	14.14
O−Si−O	107.82	94.5	109.5	94.5
CH_3−Si−CH_3	109.24	49.97	109.24	49.97
O−Si−CH_3	110.69	49.97	109.5	49.97
dihedrals	**hybrid/UA: n**	**k_t [kcal/mol]**	**UA/CI: n**	**k_t [kcal/mol]**
Si−O−Si−O	1	0.225	3	0.9006
Si−O−Si−CH_3	3	0.01	3	0.9006

angles θ_0. The Si−O−Si EA/CII potential in particular is very anharmonic, with a steep rise for angles $\theta < \theta_0$ and a small barrier followed by a steep decrease for angles $\theta > \theta_0$, which presumably leads to the large renormalization of this angle from its gas-phase value of $\theta_0 = 159°$ to its condensed phase value of $\theta_0 = 146.46°$. It is not possible to fit this anharmonic potential with a harmonic one, so we use the UA/CI values for k_θ.

The torsional potentials in the UA/CI model and the EA/CII model are quite different. Thus, for the Si−O−Si−O potential, we use eq 3 with $n = 1$ and the EA/CII value for the appropriate k_t, which is the dominant term in the EA/CII potential. For the Si−O−Si−C potential, we use the EA/CII potential, which is given by eq 3 with $n = 3$. The values of all the intramolecular potential parameters for the hybrid/UA model are given in Table 1, along with those of the UA/CI model for comparison.

The nonbond potential includes van der Waals and Coulomb interactions. These forces act between all atoms on different chains and between atoms on the same chain which are further apart than third-nearest neighbors (second-nearest neighbors for the explicit atom EA/CII potential). The nonbonded potential is defined as[1]

$$U_{\alpha\gamma}^{\text{nonbond}}(r) = \begin{cases} U_{\alpha\gamma}^{\text{vW}}(r) + k_q \dfrac{q_\alpha q_\gamma}{r} & r < r_c \\ k_q \dfrac{q_\alpha q_\gamma}{r} & r > r_c \end{cases} \quad (4)$$

where $U_{\alpha\gamma}^{\text{vW}}(r)$ are the van der Waals interactions, q is the electric charge, r is the distance between any two atoms of type α and γ, and r_c is the cutoff distance for the van der Waals interactions. We use $r_c = 12$ Å for all the simulations. The proportionality constant for the electrostatic potential energy is $k_q = 1/(4\pi\epsilon_0) = 332.06$ (kcal Å)/(e^2 mol). One of the largest differences between the UA/CI and the EA/CII models studied in ref 1 is the relative strengths of the nonbonded interactions for the Si and O atoms, which are much weaker for the EA/CII model than for the UA/CI model. As a first guess, it seems reasonable to assume that the nonbonded potentials involving the Si and O atoms should transfer directly from the EA/CII model to an accurate UA model. We therefore decided to use the EA/CII 9−6 potential for the Si, O, and Si−O van der Waals interactions:

$$U_{\alpha\gamma}^{\text{vW}}(r) = U_{\alpha\gamma}^{\text{II}}(r) = \epsilon_{\alpha\gamma}\left[2\left(\frac{\sigma_{\alpha\gamma}}{r}\right)^9 - 3\left(\frac{\sigma_{\alpha\gamma}}{r}\right)^6\right], \quad \alpha \text{ and } \gamma = \{\text{Si, O}\} \quad (5)$$

We use the EA/CII interaction parameters given in refs 2−6 for the silicon and oxygen potentials, with the usual class II mixing rules for the Si−O potential:[3]

$$\epsilon_{\text{SiO}} = \frac{2\sigma_{\text{Si}}^3\sigma_{\text{O}}^3\sqrt{\epsilon_{\text{Si}}\epsilon_{\text{O}}}}{\sigma_{\text{Si}}^6 + \sigma_{\text{O}}^6}, \quad \sigma_{\text{SiO}} = \left(\frac{\sigma_{\text{Si}}^6 + \sigma_{\text{O}}^6}{2}\right)^{1/6} \quad (6)$$

We use a standard Lennard-Jones potential for all interactions involving the methyl groups:

$$U_{\alpha\gamma}^{\text{vW}}(r) = U_{\alpha\gamma}^{\text{LJ}}(r) = 4\epsilon_{\alpha\gamma}\left[\left(\frac{\sigma_{\alpha\gamma}}{r}\right)^{12} - \left(\frac{\sigma_{\alpha\gamma}}{r}\right)^6\right], \quad \alpha \text{ or } \gamma = \text{CH}_3 \quad (7)$$

For the CH_3−CH_3 interactions, we use the parameters from the TraPPE potential.[8] We use the Berthelot mixing rule for the $\epsilon_{\alpha\gamma}$ for the Si−CH_3 and O−CH_3 interactions, $\epsilon_{\alpha\gamma} = \sqrt{\epsilon_\alpha\epsilon_\gamma}$. The minimum of the 9−6 potential in eq 5 is at $r = \sigma_{\alpha\gamma}$, whereas the minimum of the Lennard-Jones potential of eq 7 is at $r = 2^{1/6}\sigma_{\alpha\gamma}$, so that the $\sigma_{\alpha\gamma}$ for the different potentials are not equivalent. Therefore, to obtain values for the $\sigma_{\alpha\gamma}$ for the Si−CH_3 and O−CH_3 interactions, we first average the hard-core diameters

$$d_{\alpha\gamma} = (d_\alpha + d_\gamma)/2 \quad (8)$$

where d is defined by[9,10]

$$d = \int_0^{r_\infty} dr\, \{1 - \exp[-\beta U_r(r)]\} \quad (9)$$

and $U_r(r)$ is the repulsive part of the relevant potential, $U_{\alpha\gamma}^{\text{II}}(r)$ for Si or O atoms and $U_{\alpha\gamma}^{\text{LJ}}(r)$ for CH_3 groups. We then determine the value of $\sigma_{\alpha\gamma}$ needed to obtain the hard-core diameter given by eq 8. Since we are mixing 12−6 and 9−6 potentials in this model of PDMS, we refer to it as the hybrid/UA model. The nonbonded interaction parameters are listed in Table 2, along with the parameters used in the UA/CI model of Sok et al.[7] We ran several simulations with different values of the electrostatic partial charges, as will be discussed below in section III.

We note that the EA/CII potential includes nonbond interactions between third-nearest neighbors on the same chain, whereas the UA potentials do not. Third-nearest neighbors in the EA/CII model thus experience both torsional and nonbond forces, so in general one should not use the same torsional parameters for the EA/CII and UA models, as we have done. To check the validity of our torsional potential, we calculated the EA/CII nonbond van der Waals energies between atoms

involved in the torsional potential. We found that the van der Waals energy has a negligible dependence on the torsional angle ϕ for the backbone Si−O−Si−O dihedral angle (it varies by 0.010 kcal/mol from $\phi = \pi$ to $\phi = 0$, compared to the torsional energy variation of 0.47 kcal/mol). The dependence of the van der Waals energy on ϕ is slightly larger for the Si−O−Si−C dihedral angle, varying by 0.017 kcal/mol from $\phi = \pi$ to $\phi = 0$, and is a larger fraction of this torsional energy. However, this is such a small energy compared to kT, as is the torsional energy (with an amplitude of 0.02 kcal/mol), that it should have a negligible effect on the structure.[11] The bare Coulomb energies between third-nearest neighbors are considerably larger than the torsional energies. However, as we will discuss below, the Coulomb interactions appear to be considerably screened in the melt. We obtain comparably good chain dimensions for the hybrid/UA model with and without charges, when compared to the EA/CII model with and without charges, which implies that the effects of the Coulomb interactions on the torsional potential are also small. Thus, use of the EA/CII torsional potentials in the hybrid/UA model is justified. The inclusion of the nonbond forces between third-nearest neighbors would change the absolute energies somewhat due to extra additive constants but has no effect on the forces and therefore no effect on the structure of the melt. This conclusion is not general, however. For example, the nonbond potentials between third-nearest neighbors are quite significant in an explicit atom model of polyethylene,[12] so care must be taken in translating torsional potentials between explicit and united atom models.

The simulations were run using the parallel LAMMPS MD code.[13] All simulations were done on systems of 80 chains with 20 Si atoms per chain, except for the results using the EA/CII model which used systems of 100 chains of the same length (20 Si atoms per chain). Initial configurations of methyl-terminated PDMS chains were prepared as described in ref 1. Overlaps were removed using a soft nonbond potential. A time step of $\delta t = 0.4$ fs was used for most of the simulations. In all simulations we used a multiple-time step integrator (RESPA) so that forces were calculated every time step for bonded interactions, every two time steps for three- and four-body forces, and every four time steps for van der Waals and Coulomb forces. The long-range Coulomb interactions were calculated with a particle−particle/particle−mesh Ewald (PPPM) algorithm.[14] All simulations were run at a constant density of $\rho = 0.98$ g/cm^3. The temperature T was controlled with a Nose-Hoover thermostat using a coupling frequency of 0.02 fs^{-1}.

Systems were equilibrated at $T = 600$ K until the average distance traveled by the center of mass of the chains was at least twice the average radius of gyration (up to about 2.9 ns). The temperature was then lowered to 300 K, and the systems equilibrated until the chains moved one more radius of gyration. Statistics were then collected for 2.6−3 ns, sampling configurations every 0.04 ns. The simulations were run on between 16 and 32 processors on the Sandia CPlant cluster.

III. Simulation Results and Discussion

We evaluate the new hybrid/UA potential by comparing the structure of the melt, the pressure, and the chain dimensions with the results for the EA/CII model obtained by Sides et al.[1] As mentioned in the Introduction, the results of the EA/CII model are in very good agreement with experiment and thus represent a good test of the new hybrid/UA model. We calculate the intermolecular correlation functions $g_{\alpha\gamma}(r)$ defined by

$$g_{\alpha\gamma}(r) = \int \frac{\langle \rho_\alpha(\mathbf{r}')\, \rho_\gamma(\mathbf{r}) \rangle}{\rho_\alpha \rho_\gamma}\, \mathrm{d}\mathbf{r}' \tag{10}$$

where $r = |\mathbf{r} - \mathbf{r}'|$ and ρ_α is the density of sites of type α, as well as the total molecular structure factor $H(k)$, as defined in ref 1. It is clearly not possible to compare the six intermolecular correlation functions of the UA models with the 10 correlation functions of the EA models, so here we consider the six $g_{\alpha\gamma}(r)$ with H $\notin \{\alpha,\gamma\}$, and we compare correlations containing C atoms in the EA/CII model with CH_3 groups in the UA models. For the EA results, the $H(k)$ are calculated from the MD data using the CH_3 scattering form factor for all of the C sites and ignoring the direct contribution of the H sites, as was done in the experimental analysis in ref 1.

In ref 1 it was found that the Coulomb interactions have a strong effect on the structure of the melt predicted by the UA/CI model. To investigate the effect of the Coulomb interactions, we carried out simulations both with and without the Coulomb interactions. In Figure 1 we show the six intermolecular correlation functions $g_{\alpha\gamma}(r)$, calculated directly using the particle positions from the MD simulations and averaged over independent configurations. The open squares show the results for the EA/CII model with Coulomb interactions using the partial charges listed in Table 4,[1] the open diamonds are for the EA/CII model with all charges $q = 0$, and the solid curve shows the MD results for the hybrid/UA model, also with all $q = 0$. We see that the Coulomb interactions have relatively little effect on the intermolecular structure predicted by the EA/CII model. Furthermore, the hybrid/UA model is in fairly good agreement with the EA/CII results. The hybrid/UA model with $q = 0$ tends to underpredict the low-r peaks in the Si−Si, O−O, and Si−O correlations, but the peak positions are well fit as is the overall shape of the $g_{\alpha\gamma}(r)$. Figure 2 compares the results for the structure factor $H(k)$ for the same models. The main effect of the Coulomb interactions in the EA/CII model seems to be to increase the height of the first peak and lower the height of the second peak. The hybrid/UA model with $q = 0$ is again a good fit to the EA/CII model with no charges and a reasonable fit to the full EA/CII model with charges. The agreement at high k is excellent. The total structure factor at $k = 0$ is related to the bulk isothermal compressibility κ_T by

$$H(0) = k_B T \rho \kappa_T - 1 \tag{11}$$

Thus, the larger value of $H(0)$ predicted by the hybrid/UA model compared to the EA/CII model indicates a somewhat larger compressibility in the hybrid/UA model.

Since the charges had relatively little effect on the EA/CII model, one might hope to obtain a similar result for the UA model. Thus, we ran simulations using the same partial charges as for the EA/CII model for the Si and O atoms, $q_{Si} = 0.715$ and $q_O = -0.445$, and simply added the C and H charges to obtain the methyl group charge, $q_{CH_3} = q_C + 3q_H = -0.135$ (see Tables 3 and 4). The partial charges of the Si atoms on the ends of the

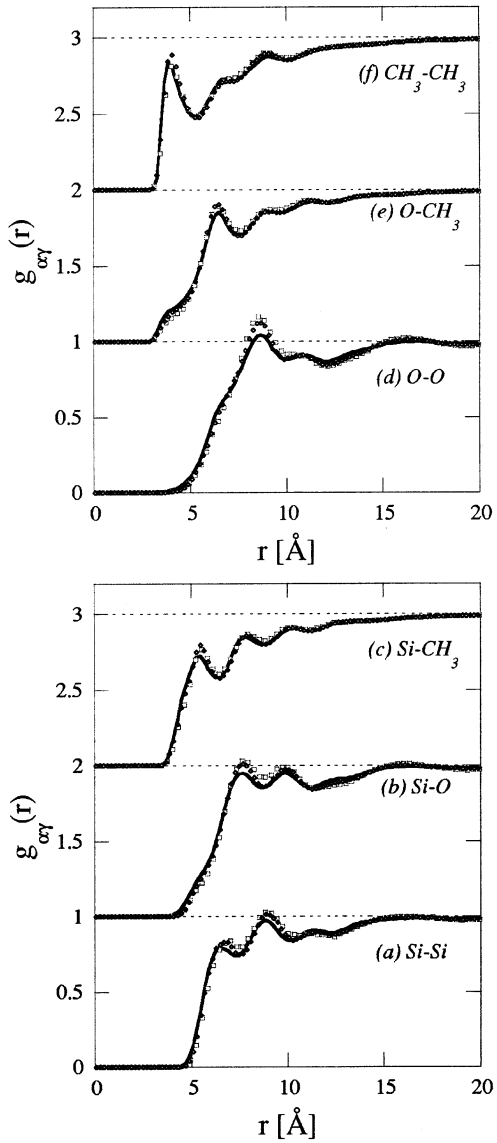

Figure 1. Comparison of intermolecular correlation functions $g_{\alpha\gamma}(r)$ using the EA/CII model with charges (open squares), the EA/CII model with $q = 0$ (diamonds), and the hybrid/UA model with $q = 0$ (solid curves). The values of $g_{\alpha\gamma}(r)$ in each panel have been offset for clarity.

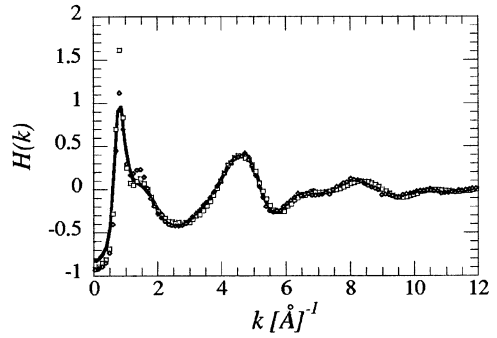

Figure 2. Comparison of $H(k)$ using the EA/CII model with charges (open squares), the EA/CII model without charges (diamonds), and the hybrid/UA model without charges (solid curves).

chains were adjusted to preserve overall chain neutrality. The results for the $g_{\alpha\gamma}(r)$ are shown as the dotted curves in Figure 3. For the UA model the charges have a large effect on the intermolecular structure. In particular, with the partial charges turned on there is much more short-ranged structure in all the correlations except those for Si−CH_3 and CH_3−CH_3. The same effect can also be seen in $H(k)$, as shown as the dotted curve in Figure 4. Most significantly, the first peak is shifted to larger k. Thus, the hybrid/UA model with the EA/CII partial charges actually gives a worse fit to the full EA/CII results than does the hybrid/UA model without Coulomb interactions.

Table 2. Van der Waals Interaction Parameters for the Hybrid/UA and UA/CI Models

	hybrid/UA: ϵ [kcal/mol]	σ [Å]	UA/CI: ϵ [kcal/mol]	σ [Å]
Si−Si	0.1310	4.29	0.5848	3.385
Si−O	0.0772	3.94	0.3462	3.170
Si−CH_3	0.1596	3.83	0.3244	3.586
O−O	0.0800	3.30	0.2049	2.955
O−CH_3	0.1247	3.38	0.1920	3.371
CH_3−CH_3	0.1944	3.73	0.1799	3.786

Since the charges have so little effect on the intermolecular structure predicted by the EA/CII model, they must be well screened in the condensed melt phase. To examine this effect more closely, we calculated the total charge density surrounding a given atom, due to the atoms on other chains (i.e., an "intermolecular" charge density):

$$\rho_{e,\alpha}(r) = \frac{1}{\rho}\sum_{\gamma} q_\gamma \langle n_{\alpha\gamma}(r)\rangle_\alpha \qquad (12)$$

where $n_{\alpha\gamma}(r)$ is the density of atoms of type γ located on a different chain at a distance r from the atom of interest of type α. The average is over all atoms of type α (so that the quantity $\langle n_{\alpha\gamma}(r)\rangle_\alpha$ is proportional to $g_{\alpha\gamma}(r)$), and we have normalized by the total site density ρ. We show $\rho_e(r)$ for all three atom types in Figure 5, where open squares are the results for the EA/CII model and the dotted curves are the results for the hybrid/UA model with EA/CII charges. As anticipated, the charge density around any given atom is much less screened in the hybrid/UA model. This must be due to the lack of the hydrogen atoms. In the EA/CII model, the H atoms have small positive charges, while the C atoms have negative charge. The positive charges on the H atoms are able to screen somewhat the negative charges on the C and probably the O atoms. For example, the curves for $\rho_{e,O}$ in Figure 5b show that for the EA/CII model there is a small positive charge due to H atoms on neighboring chains near the oxygens, followed by a small negative charge due to the C atoms. In the corresponding hybrid/UA curves, because of the lack of the hydrogen atoms, there is a large negative charge due to negatively charged methyl groups near the oxygen atoms. Similarly, for the C atoms in the EA/CII model, the nearby negative oxygens are screened somewhat by the H atoms on the methyl group, whereas this does not occur for the hybrid/UA model.

It is also instructive to compare the pressure and chain dimensions obtained with the different models. The pressure P, the radius of gyration R_g, and the end-to-end distance R_{ee} (defined by a terminal silicon atom and one of the methyl groups on the opposite end of the chain), along with the relevant partial charges, are tabulated for the hybrid/UA and the UA/CI models in Table 3 and for the EA/CII model in Table 4. For now we focus on the first three lines in Table 3. The pressure is lower in the hybrid/UA model than in the EA/CII model, although both are near zero. With the charges

Table 3. Partial Charges, Pressure, Mean-Squared Radius of Gyration, and End-to-End Distance for the Hybrid/UA and the UA/CI Models[a]

model	q_{Si}	q_O	q_{CH_3}	P [atm]	$\langle R_g^2 \rangle$ [Å^2]	$\langle R_{ee}^2 \rangle$ [Å^2]
hybrid/UA	0	0	0	-182.5 ± 18.1	78.4 ± 0.2	492.3 ± 2.6
UA/CI	0	0	0	-1013.6 ± 47.2	72.4 ± 0.6	439.0 ± 13.7
hybrid/UA	0.715	−0.445	−0.135	-67.3 ± 20.1	75.7 ± 0.2	411.5 ± 2.0
hybrid/UA	0.445	−0.445	0	-287.3 ± 18.2	100.5 ± 0.1	641.6 ± 2.6
hybrid/UA	0.3	−0.3	0	-167.0 ± 18.0	90.3 ± 0.3	568.3 ± 4.4
UA/CI	0.3	−0.3	0	-963.0 ± 35.5	80.6 ± 0.3	498.9 ± 6.8

[a] Note: the pressure values do not include tail corrections.

Table 4. Partial Charges, Pressure, Mean-Squared Radius of Gyration, and End-to-End Distance for the EA/CII Model[a]

model	q_{Si}	q_O	q_C	q_H	P [atm]	$\langle R_g^2 \rangle$ [Å^2]	$\langle R_{ee}^2 \rangle$ [Å^2]
EA/CII	0	0	0	0	685.9 ± 35	81.5 ± 0.2	523.0 ± 3.0
EA/CII	0.715	−0.445	−0.294	0.053	190.9 ± 53.2	92.6 ± 2.4	672.2 ± 32.3

[a] Note: the pressure values do not include tail corrections.

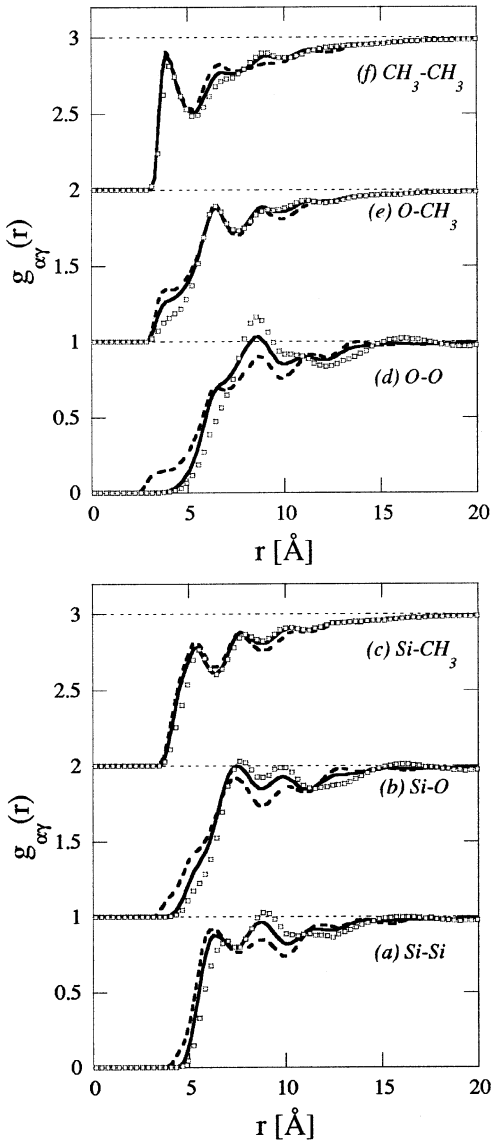

Figure 3. Comparison of intermolecular correlation functions $g_{\alpha\gamma}(r)$ using the EA/CII model with charges (open squares), the hybrid/UA model with EA/CII charges $q_{Si} = 0.715$, $q_O = -0.445$, and $q_{CH_3} = -0.135$ (dotted curves), and the hybrid/UA model with $q_{Si} = -q_O = 0.3$ and $q_{CH_3} = 0$ (solid curves).

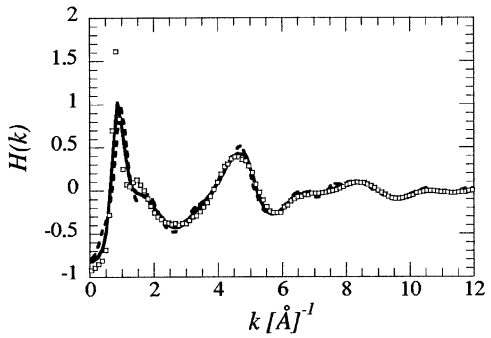

Figure 4. Comparison of $H(k)$ using the EA/CII model with charges (open squares), the hybrid/UA model with charges $q_{Si} = 0.715$, $q_O = -0.445$, and $q_{CH_3} = -0.135$ (dotted curves), and the hybrid/UA model with $q_{Si} = -q_O = 0.3$ and $q_{CH_3} = 0$ (solid curves).

set to zero, the chain dimensions of the hybrid/UA model are in better agreement with the EA/CII model than are those of the UA/CI model. The asymmetry of the chains with all $q = 0$ is similar for all three models: the ratios of the moments of inertia $\langle R_{g1}^2 \rangle : \langle R_{g2}^2 \rangle : \langle R_{g3}^2 \rangle$ are 1.0:2.72:12.58 for the hybrid/UA model, 1.0:2.72:13.01 for the EA/CII model, and 1.0:2.35:12.69 for the UA/CI model (note that for an ideal random walk the ratios are 1.0:2.5:11.8[15]). In the EA/CII model, including the charges leads to a decrease in pressure, whereas in the hybrid/UA model the charges give an increase in pressure. This implies that in the EA/CII model the net effect of the Coulomb interactions is attractive, while in the hybrid/UA model the net effect is repulsive. Interestingly, although the charges have a small effect on the intermolecular structure predicted by the EA/CII model, they have a much larger effect on the chain dimensions, causing an increase in $\langle R_g^2 \rangle$ of about 14% due to intramolecular, Coulombic repulsions. For the hybrid/UA model, the charges have a smaller effect on $\langle R_g^2 \rangle$ and in the opposite direction, giving a smaller chain rather than an expanded chain as one might have expected.

To better approximate these effects of the screening, we did further simulations of the hybrid/UA model with the charge on the methyl group set to zero, $q_{CH_3} = 0$. We first kept the charge on the O atoms the same as in the EA/CII model, $q_O = -0.445$, so that $q_{Si} = 0.445$ for charge neutrality. As can be seen in Table 3, this leads to a much larger $\langle R_g^2 \rangle$ than is obtained for the EA/CII model. Furthermore, it only improved the predictions for the structure by a small amount. However, the trends in chain dimension and pressure with charge are now the same as in the EA/CII model, so that setting $q_{CH_3} = 0$ does mimic some of the effects that the positive hydrogens have in screening the negative C charge in the EA/CII model. Thus, to further reduce the effects

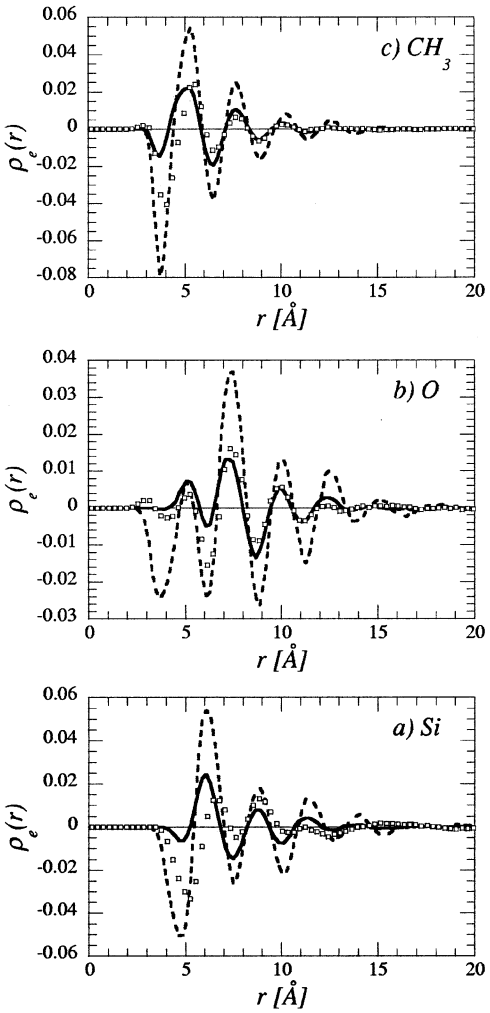

Figure 5. Total intermolecular charge density distributions around the (a) Si atoms, (b) O atoms, and (c) CH_3 (or C) atoms. Symbols denote the EA/CII model with charges (open squares), the hybrid/UA model with $q_{Si} = 0.715$, $q_O = -0.445$, and $q_{CH_3} = -0.135$ (dotted curves), and the hybrid/UA model with $q_{Si} = -q_O = 0.3$ and $q_{CH_3} = 0$ (solid curves).

of the charge, we lowered the values of q_{Si} and $-q_O$ until we obtained approximately the same chain dimensions as the EA/CII model predicts. We found that values of $q_{Si} = -q_O = 0.4$ were still too large, $q_{Si} = -q_O = 0.3$ gave $\langle R_g^2 \rangle$ close to the EA/CII value, and values of $q_{Si} = -q_O = 0.15$ were sufficiently small as to give results that were almost indistinguishable from the case of zero partial charges.

Thus, we focus on the case with $q_{Si} = -q_O = 0.3$. Interestingly, these are precisely the partial charges used in the UA/CI model of Sok et al. (see Table 3). The predicted $g_{\alpha\gamma}(r)$ and $H(k)$ are shown as the solid curves in Figures 3 and 4, respectively. Although the predicted intermolecular structure still disagrees with that of the EA/CII model, the fit is much closer than with the partial charges equal to their values for the EA/CII model. In particular, the fit of the experimentally measurable $H(k)$ is reasonably good. We show this more clearly in Figure 6, which shows the wide-angle X-ray scattering data from ref 1, along with the MD results for the EA/CII and the hybrid/UA model with $q_{Si} = -q_O = 0.3$ and $q_{CH_3} = 0$. We see from the solid curves in Figure 5 that the total charge density around any given atom is much smaller with $q_{Si} = -q_O = 0.3$ and $q_{CH_3} = 0$ in the hybrid/UA model. Finally, for this case the chain

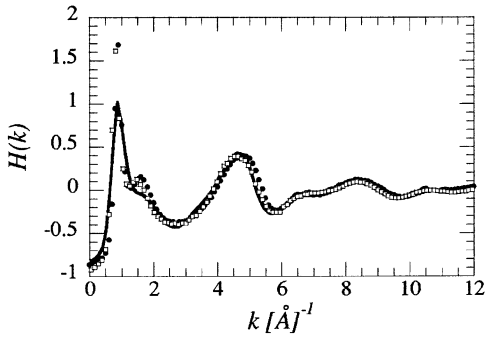

Figure 6. Structure factor $H(k)$ as obtained from wide-angle X-ray scattering in ref 1 (solid circles), the EA/CII model with charges (open squares), and the hybrid/UA model with $q_{CH_3} = 0$ and $q_{Si} = -q_O = 0.3$ (solid curves).

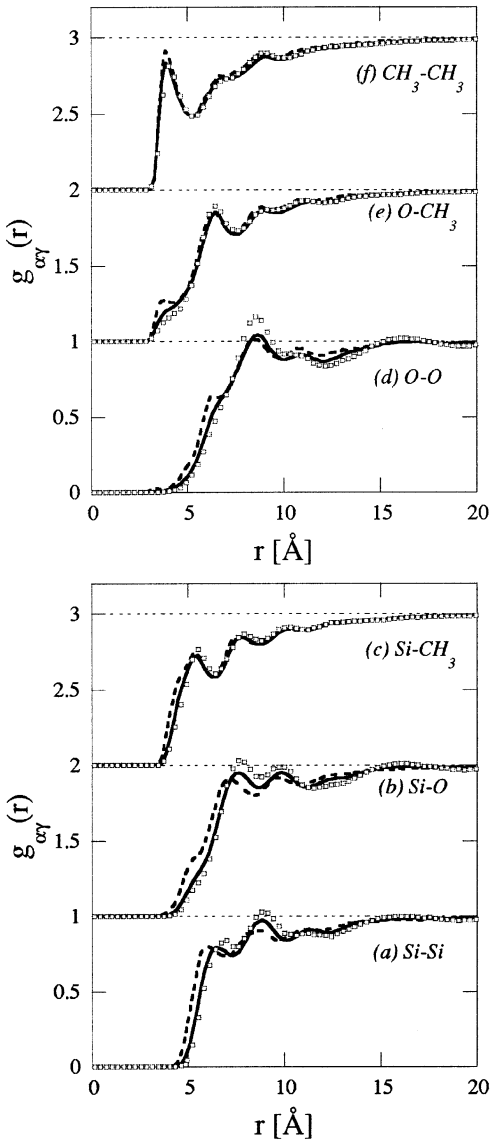

Figure 7. Comparison of intermolecular correlation functions $g_{\alpha\gamma}(r)$ using the EA/CII model with charges (open squares), the UA/CI model of Sok et al.[7] with $q = 0$ (dotted curves), and the hybrid/UA model with $q = 0$ (closed curves).

dimensions are in better agreement with the EA/CII results. While the value of $\langle R_{ee}^2 \rangle$ is about 15% lower than the EA/CII value, the values of $\langle R_g^2 \rangle$ agree quite well.

Significant further improvements seem unlikely with a united atom model. It seems that including the hydrogen atoms explicitly is crucial for modeling all of

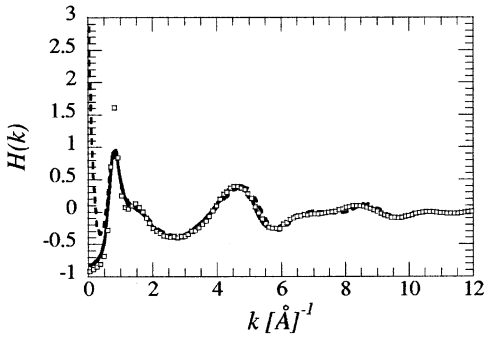

Figure 8. Comparison of $H(k)$ using the EA/CII model with charges (open squares), the UA/CI model with $q = 0$ (dotted curves), and the hybrid/UA model with $q = 0$ (closed curves).

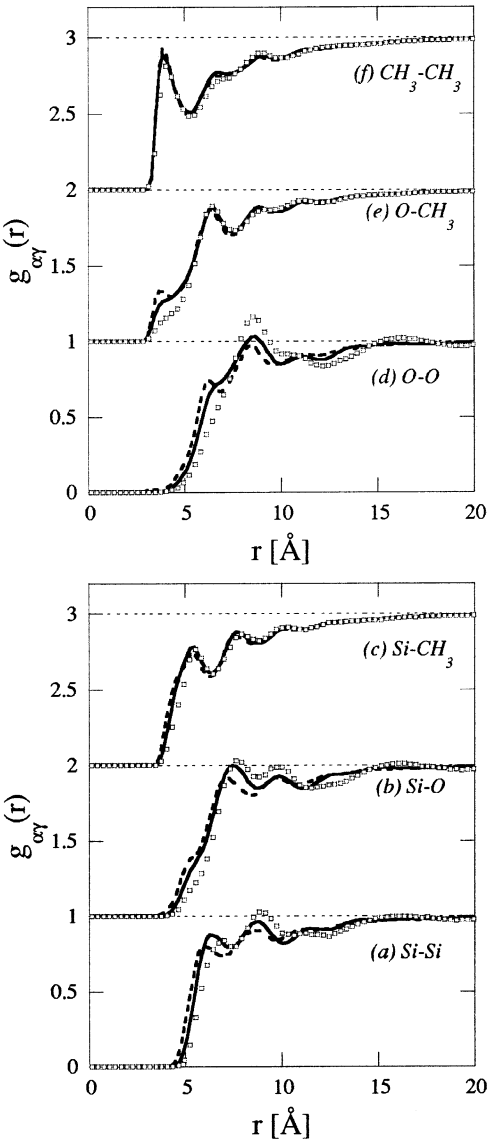

Figure 9. Comparison of intermolecular correlation functions $g_{\alpha\gamma}(r)$ using the EA/CII model with charges (open squares), the UA/CI model with charges (dotted curves), and the hybrid/UA model with $q_{CH_3} = 0$ and $q_{Si} = -q_O = 0.3$ (solid curves).

the details of the structure and chain dimensions of PDMS, since the hydrogen atoms play a very important role in screening the charge density in the melt state. It might be possible to better mimic the effects of the screening by using screened Coulomb interactions rather than the bare Coulomb interactions of eq 4. The pressure could be increased by shortening the range of the attractive tail of one or more of the van der Waals interactions. Better agreement with the EA/CII model might also be achieved by adjusting the Si−CH_3 and O−CH_3 interactions. However, it is unclear how to implement these ideas in a systematic fashion.

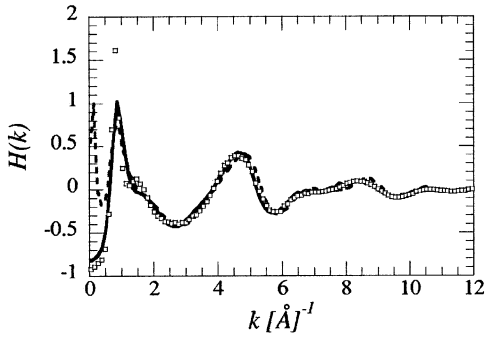

Figure 10. Comparison of $H(k)$ using the EA/CII model with charges (open squares), the UA/CI model with charges (dotted curves), and the hybrid/UA model with $q_{CH_3} = 0$ and $q_{Si} = -q_O = 0.3$ (solid curves).

Nevertheless, the hybrid/UA model developed here gives a better representation of the properties of PDMS than does the previously available UA/CI model of Sok et al. First of all, as seen in Table 3, the UA/CI model predicts much smaller chain dimensions than the hybrid/UA model. Furthermore, it predicts a large negative pressure, which as discussed in ref 1 implies that the liquid/gas transition for the UA/CI model is too high. The pressures obtained with the hybrid/UA model are much more reasonable, although still negative. We compare the $g_{\alpha\gamma}(r)$ and $H(k)$ for the two united atom models, both with and without charges, in Figures 7−10. The hybrid/UA model without charges gives a much closer fit to the intermolecular correlations predicted by the EA/CII model than does the UA/CI model. The hybrid/UA model also avoids the anomalous turn up in $H(k)$ at low k exhibited by the UA/CI model due to its high compressibility. Thus, for applications in which the intermolecular structure is the most important feature, the hybrid/UA model with $q = 0$ should give very good results. As shown in Figures 9 and 10, the hybrid/UA model with $q_{Si} = -q_O = 0.3$ does a slightly better job of predicting structure than does the UA/CI model with the same partial charges. In this case the main advantages of the hybrid/UA model are its much improved compressibility (as seen in the low-k behavior of $H(k)$ and the pressure) and its improved chain dimensions. We therefore recommend the hybrid/UA model with q_{CH_3} and $q_{Si} = -q_O = 0.3$ for any applications in which the chain dimensions play a significant role.

In conclusion, we have developed a new united atom force field for computer simulations of PDMS based on a successful explicit atom model studied previously. In comparison with the EA results of Sides et al.,[1] the hybrid/UA model presented here gives an excellent description of the structure of PDMS in the absence of partial charges. We found that the hydrogen atoms play an important role in screening the charges in the EA/CII model. These screening effects can be partially accounted for in the UA model by taking the charge on the methyl groups to be zero and by reducing the charges on the Si and O atoms from the values used in the EA/CII model. The resulting hybrid/UA model, with $q_{CH_3} = 0$ and $q_{Si} = -q_O = 0.3$, gives relatively good

agreement with the EA/CII model for the structure, pressure, and chain dimensions of PDMS melts.

Acknowledgment. We thank Scott Sides for many helpful discussions and for data on the EA/CII model and Gary Grest for helpful discussions. Sandia is a multiprogram laboratory operated by Sandia Corporation, a Lockheed Martin Company, for the United States Department of Energy under Contract DE-AC04-94AL85000.

References and Notes

(1) Sides, S. W.; Curro, J. G.; Grest, G. S.; Stevens, M. J.; Soddemann, T.; Habenschuss, A.; Londono, J. D. *Macromolecules* **2002**, *35*, 6455.
(2) Hwang, M. J.; Stockfisch, T. P.; Hagler, T. A. *J. Am. Chem. Soc.* **1993**, *116*, 2515.
(3) Maple, J. R.; Hwang, M. J.; Stockfisch, T. P.; Dinur, U.; Waldman, M.; Ewig, C. S.; Hagler, A. T. *J. Comput. Chem.* **1994**, *15*, 162.
(4) Sun, H. *Macromolecules* **1995**, *28*, 701.
(5) Sun, H.; Rigby, D. *Spectrochim. Acta, Part A* **1997**, *53*, 1301.
(6) Sun, H. *J. Phys. Chem. B* **1998**, *102*, 7338.
(7) Sok, R. M.; Berendsen, H. J. C.; van Gunsteren, W. F. *J. Chem. Phys.* **1992**, *96*, 4699.
(8) Martin, M. J.; Siepmann, J. I. *J. Phys. Chem. B* **1999**, *103*, 4508.
(9) Hansen, J.; McDonald, I. *Theory of Simple Liquids*; Academic Press: London, 1986.
(10) Barker, J. A.; Henderson, D. *J. Chem. Phys.* **1967**, *47*, 4714; *Annu. Rev. Phys. Chem.* **1972**, *23*, 439; *Rev. Mod. Phys.* **1976**, *48*, 587.
(11) Since the value of k_t for the Si−O−Si−C dihedral angle is so small, it must not have any effect on the structure and could have been taken to be zero. We kept the value of $k_t = 0.01$ to be consistent with the EA/CII potential parameters from ref 5.
(12) Tsige, M.; Curro, J. G.; Grest, G. S.; McCoy, J. D. Submitted to *Macromolecules*.
(13) Plimpton, S. J. *J. Comput. Phys.* **1995**, *117*, 1−19.
(14) Hockney, R.; Eastwood, J. *Computer Simulations Using Particles*; Adam Hilger: New York, 1988.
(15) Kremer, K.; Grest, G. S. *J. Chem. Phys.* **1990**, *92*, 5057.

MA025763G